Applied Thermal Engineering 82 (2015) 306–317

Contents lists available at ScienceDirect

Applied Thermal Engineering

journal homepage: www.elsevier.com/locate/apthermeng

Research paper

A comparative performance study of a direct expansion geothermal evaporator using R410A and R407C as refrigerant alternatives to R22

Jean-Louis Comlan Fannou*, Clément Rousseau, Louis Lamarche, Stanislaw Kajl

Thermal Technology Center (TTC), Department of Mechanical Engineering, École de Technologie Supérieure, Université du Québec, 1100, Notre-Dame Street West, Montreal, QC H3C 1K3, Canada

HIGHLIGHTS

- Direct expansion geothermal evaporator has been simulated using R22, R410A and R407C.
- R407C is the best fluid for retrofit R22 system in the field of DX GHP.
- The pressure drop in R407C DX evaporators is higher than that of R410A.
- The pressure drop in R22 DX evaporator is higher than those of R407C and R410A.
- HER does not really depend to the type of refrigerant at a given soil temperature.

ARTICLE INFO

Article history:
Received 7 December 2014
Accepted 27 February 2015
Available online 9 March 2015

Keywords:
Geothermal heat pump
DX evaporator
Pressure drop
Superheating
R410A
R407C

ABSTRACT

This study presents a comparative performance analysis of a direct expansion geothermal evaporator using R410A, R407C and R22 as refrigerants. The main goal is to predict the best refrigerant capable of serving as a substitute for R22. A validated geothermal evaporator model developed by our research team was used. The simulation results show that for low refrigerant flow rate, the R410A DX evaporator shows better performance than that of R22, but from the pressure drop observed and superheating recorded with the former, it can be concluded that R407C is the best fluid to replace R22 in the DX GHP. That notwithstanding, to minimize pressure drop, especially for high refrigerant flow rates, R410A would be a better choice for the design of new DX systems.

1. Introduction

With the coming into force of the Montreal Protocol in 1989, the most environmentally harmful refrigerants, such as CFCs (Table 1), have been banned since 1995 [8]. Those less damaging to the ozone layer, such as HCFCs (Table 1) have a replacement schedule extending until 2040 [24]. R22 shall be replaced by HFCs to as Montreal Protocol. Thus, to overcome these protocol challenges, several studies are ongoing in various fields, and are summarized in Fig. 1 [1,2,4,5,6,7,9,12,15,16,21,22,23,25,27,29,31,32,33,35,36,39,40,42,43,45,48,49,50].

These studies aim mainly to:

- Develop new refrigerants to be prioritized [15,41].
- Develop new heat transfer coefficient expressions [28,52].
- Define tools for analyzing new and existing systems (including components) with respect to fluid substitution.
- Choose the best refrigerant performing similarly to or better than R22.
- Develop the best strategies for system retrofit, including the choice of lubricating oil, while ensuring performance, safety and environmental protection.

Several methods have been developed to synthesize and produce new refrigerants capable of replacing R22. Specifically with respect to air conditioning and heat pumps, the substitute refrigerants currently available on the market are: R134a, R404A, R410A, R407C, R1270, CO_2 (R744) etc. ([26,53,54]), as well as future generation options discussed by James M. Calm [17] and Yunho et al. [8].

* Corresponding author. Tel.: +1 514 396 8858.
E-mail addresses: jean-louis-comlan.fannou.1@ens.etsmtl.ca, jlfannou@gmail.com, jean-louis.fannou.1@ens.etsmtl.ca (J.-L.C. Fannou), clement.rousseau.2@ens.etsmtl.ca (C. Rousseau), louis.lamarche@etsmtl.ca (L. Lamarche), stanislaw.kajl@etsmtl.ca (S. Kajl).

http://dx.doi.org/10.1016/j.applthermaleng.2015.02.079
1359-4311/

Nomenclature

h_{tot}	Global heat transfer coefficient ($Wm^{-2}K^{-1}$)
T_{cr}	Critical temperature (°C)
P_{cr}	Critical pressure (kPa)
d_e	Evaporation distance in the borehole (m)
T_{sol}	Ground temperature (°C)
P	Pressure (kPa)
h	Specific enthalpy (J/kg)
hg	Vapor specific enthalpy (J/kg)
hf	Liquid specific enthalpy (J/kg)
M_{wt}	Molecular weight (kg $mol^{-1}K^{-1}$)
HOC	Heat of Combustion (MJ kg^{-1})
NBP	Normal Boiling Point (°C)
LFL	Lower Flammability Limit (%)
k_s	Ground thermal conductivity((W/m.K)
Cp_s	Ground specific heat (J/kg.K)
ρ_s	Ground density (kg/m^3)
H_s	Heat transfer coefficient between pipe and grout ($W.m^{-2}.K^{-1}$)
DX	Direct Expansion
SL	Secondary Loop
PDE	Partial differential equations
HT	Heat transfer in solid
ODP	Ozone Depletion Potential
GWP	Global Warming Potential
GHP	Geothermal Heat Pump
GHE	Geothermal Heat Exchanger
NIST	National Institute of Standards and Technology
CFCs	ChloroFluoroCarbons
Tc_{mean}	Mean temperature of grout (°C)
COP	Coefficient of performance of heat pump
HFC	HydroFluoroCarbon
HCFC	HydroChloroFluoroCarbon
HER	Heat Extract Rate (Wm^{-1})

Many studies have been carried out as well on heat exchangers and on the overall heat pump to assess their performance versus fluids serving as candidates to replace R22, and to develop strategies for the conversion of heat pump systems currently in service, most of them operating with R22. The results vary with the experimental conditions, the design, the refrigerant and the systems used. Readers may refer to Fig. 1 for more details.

The alternative refrigerants to R22 evaluated vary significantly: (*i*) R407C and R410A in a 10.5 kW residential heat pump [3]; (*ii*) R134a, R290, R407C and R407C in a theoretical vapor compression cycle model [55]; (*iii*) R407A and R407C in a domestic heat pump [37]; (*iv*) R134a and various mixtures of R22/R134a in a domestic heat pump [44]; (*v*) R22, R134a, R290, R600, R404A, R407A, R407B, R407C, 407D, R410A, R410B, and R417A in residential air conditioners (simulation NIST software Cycle_D) [24]; (*vi*) the mixture of R290/R600/R123 in a geothermal heat pump system [14]; (*vii*) R134a in the experimental direct expansion ground-coupled heat pump (DX-GCHP); (*viii*) CO_2 in a direct expansion geothermal evaporator model [46], etc. The results obtained vary greatly, and are usually measured against those of R22, which are considered as the reference. The following are some interesting conclusions concerning air-to-air systems:

- It is possible to replace R22 by R407C because they have a neighboring thermodynamic property [3,51,53].
- The use of R410A has required that the original reciprocal compressor be changed to a smaller displacement scroll compressor (approximately 66% of R22 capacity) to achieve the same cooling capacity of R22 [3].
- Systems using R410A experience more pronounced performance degradation than those using R22, R407C, R290 and R134a because of the low critical temperature of R410A [55].
- The mixture ratio affects the COP (ratio between the heating capacity and the power consumption of the compressor) significantly, and the COP could be improved by using R134a or an appropriate mixture of R134a/R22 instead of pure R22 [44].
- R404A, R507, R407C, R427A and R422D are used to retrofit R22, and compressor tests with these fluids reveal a drop in performance of about 5–15% compared to R22 [19].
- The electric consumption values of units operating with R404A, R407C, and R410A are about 22–31% higher versus the case with R22. For the units operating with R407A, R407B, R407D, R407E, and R410B, the electric consumption is about 10–23% higher. For R600, the consumption is 6–8% higher than with R22. For all these fluids, the COP is 7–24% lower than with R22, except for R600, for which the COP is higher by 7–9%, and R134a and R290, which exhibit the same COP as R22 [24].
- When considering thermal and environmental parameters, R290 is identified as the best candidate for R22, provided the safety aspects are resolved [24].

Table 1
Environmental effects of refrigerants [8].

Refrigerants		ODP	GWP
CFCs	R11	1	3800
	R12	1	8100
HCFCs	R22	0.055	1500
	R141b	0.11	630
	R142b	0.065	2000
HFCs	R32	0	650
	R125	0	2500
	R134a	0	1300
	R407C	0	1520
	R410A	0	1725
Natural refrigerants	R744	0	1
	R717	0	0
	R600a	0	3
	R290	0	3

In the field of geothermal heat pumps, and especially that of DX heat pumps systems [56], most of the experimental work and modeling (see Fig. 1) are usually carried out with only one replacement fluid. Wang et al. [10], for example, conducted an experimental performance evaluation of a direct expansion ground-coupled heat pump (DX-GCHP) system in heating mode that uses R134a as the refrigerant. During the on–off operations, the heat pump supplied hot water to the fan-coil at 50.4 °C, and its heating capacity was 6.43 kW. The COP values of the heat pump and of the whole system were found respectively to be 3.55 and 3.28 on average at an evaporating temperature of 3.14 °C and a condensing temperature of 53.41 °C. The authors also discussed some practical points such as: (i) the heat extraction rate from the ground, (ii) refrigerant charge, and (iii) two possible new configurations to deal simultaneously with the misdistribution and instability of parallel GHE evaporators. Cerit and Erbay [18] evaluated the roll bond evaporator design which gives maximum COP for the direct

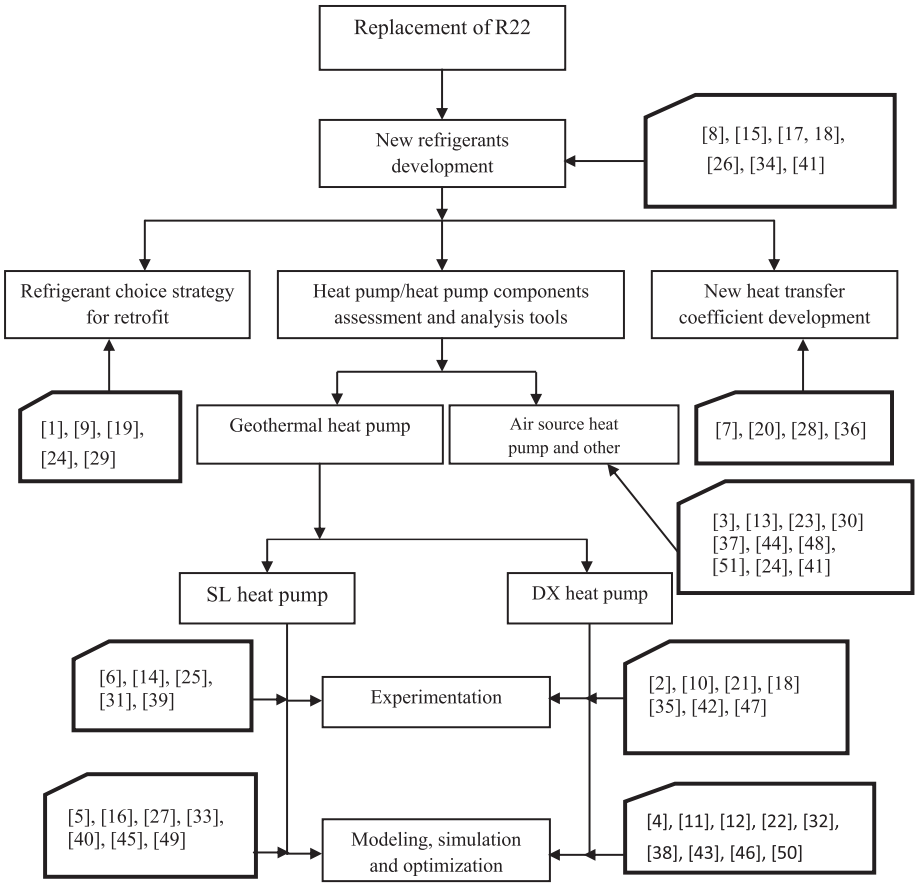

Fig. 1. Summary of the literature on replacing R22 with working field.

expansion solar-assisted heat pump (DX-SAHP) water heater investigated experimentally on three separate heat pump systems using R134a as refrigerant. The COP of the system obtained was between 2.42 and 3.3. The R407C DX heat pump was tested by Mustafa Omer [38], and performed remarkably. A direct geothermal expansion evaporator model and experimental heat pump using CO_2 as refrigerant were carried out respectively by Eslami-Nejad et al. [46] and Austin et al. [11]. As we can see in the examples cited above, these studies of the DX heat pump with R22 fluid replacements are limited to evaluating performance without carrying out a simultaneous comparative study with the R22. As highlighted by Kim et al. [30], to maintain and improve the current performance of air conditioning systems and heat pumps, an evaluation of the behavior and performance of each component, whether new or existing, with these refrigerants that are R22 alternatives should be clarified. That is why in this study, the parametric analysis of a direct expansion geothermal evaporator (Fig. 2) with three refrigerants, R22, R410A and R407C, is discussed. The aim is to determine the best R22 substitute fluid and its implications. R22 is pure refrigerant whereas R410A and R407C are zeotropic mixtures in which the temperature glide is observed during the phase change. The temperature glide is about 7 °C for R407C, versus about 0.3 °C for R410A. Thus, R410A is considered as a near-azeotropic fluid. In all cases, this temperature glide causes variations in the thermodynamic properties, and therefore a variation in the heat transfer behavior when evaporation and condensation occur. Table 2 shows the composition, physical properties and safety classifications of the fluids selected in this study.

The direct expansion geothermal evaporator (Fig. 2a) is a component of a particular heat pump generally known as a direct expansion geothermal heat pump (DX GHP) [57,58]. Heat transfer occurs directly between the refrigerant and the soil. The phase change phenomenon then occurs inside the copper tube installed on the ground. In the heat exchanger installed on a secondary loop (SL) geothermal heat pump (Fig. 2b), the heat transfer occurs between the refrigerant and other secondary fluids, such as water glycol mixture, methyl propane, etc.

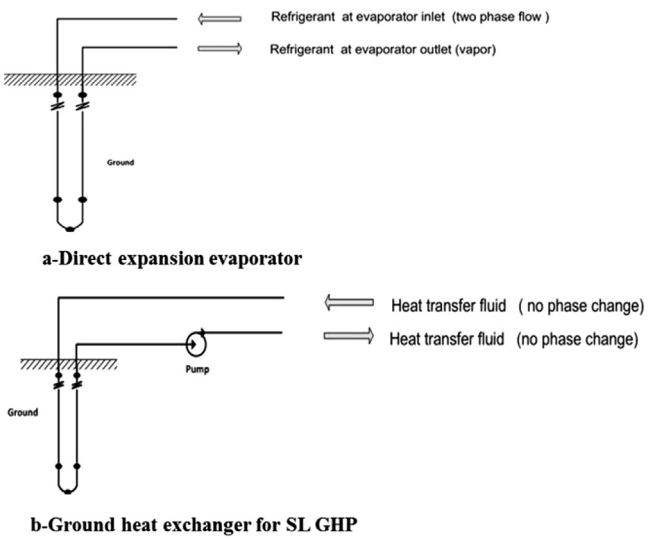

Fig. 2. Ground heat exchanger.

Table 2
Physical and safety data of the selected refrigerants [24].

Refrigerant		Physical property				Safety data		
Chemical & blend		M_{Wt}	NBP	T_{cr}	P_{cr}	ASHRAE	HOC	LFL
Composition		(kg/mol)	(°C)	(°C)	(kPa)	safety group	(MJ/kg)	
R22	$CHClF_2$	86.47	−40.8	96.1	4990	A1	2.2	none
R407C	R32/R125/ R134a	86.2	−43.8/-36.7	85.8	4600	A1	−4.9	none
R410A	R32/R125	72.58	−51.3	70.5	4810	A1	−4.4	none

2. Model used

The model used in this study and that in the global scheme shown in Fig. 3 were developed by our research team. This model was validated with R22 experimental data. It should be noted that the heat transfer coefficients correlations are adjusted to take into account both pure and mixture refrigerants used in this study. Details concerning governing equations, correlations and assumptions and validation used can be consulted in Refs. [57,59,60].

The model is devised in four domains:

- The refrigerant flow, both ascending and descending, in one dimension (z);
- The pipe, both ascending and descending, in one dimension (z);
- The grout, in one dimension (z);
- The ground, in two dimension (x,y) (Fig. 4) described as follows:

The ground temperature Ts is calculated with a two-dimensional model,

$$\rho_s Cp_s \frac{dT_s}{dt} = k_s \frac{\partial^2 T_s}{\partial x^2} + k_s \frac{\partial^2 T_s}{\partial y^2} \quad (1)$$

with at the contact between the ground and the borehole:

$$n(-k_s \nabla T_s) = H_s(T_{c_{mean}} - T_s) \quad (2)$$

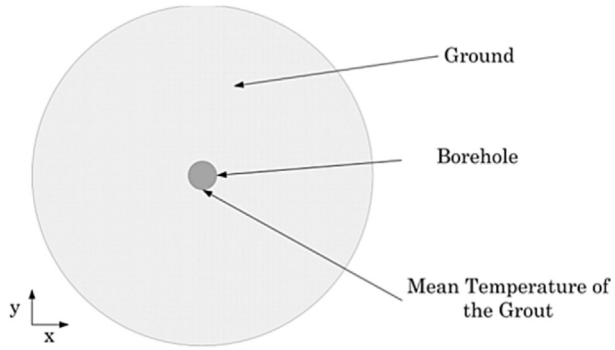

Fig. 4. Two-dimensional model of the ground.

The interest in using a two-dimensional model lies in the fact that it makes it possible to take into account the effect of a borehole to an over one.

The entire model was implemented in the Comsol software environment. Table 3 shows the model parameters. The governing equations are solved in Comsol using two modules whose variables are coupled through the boundary conditions: the PED module (resolution of mass conservation, energy conservation and momentum conservation equations) and the HTS module to solve heat transfer phenomenon in the tube, into the ground and grout. The Comsol normal mesh in one dimension was used to the ascending and descending flows with a step of 0.5 m (80 elements). The triangular mesh was used for 2-D model of the ground, with a number of 1424 elements (Fig. 5). During the simulation, the time step adopted is 10s.

Phase change zone is described by a phase-separated pattern. The local heat transfer coefficient is calculated using the superposition method based on the sum of the contributions of nucleate boiling and convective boiling [61]. The transition from the two-phase flow (inlet vapor quality is 0.2) to single-phase flow is modeled in Comsol by user-defined functions. For example, the vapor quality is determined in Comsol by:

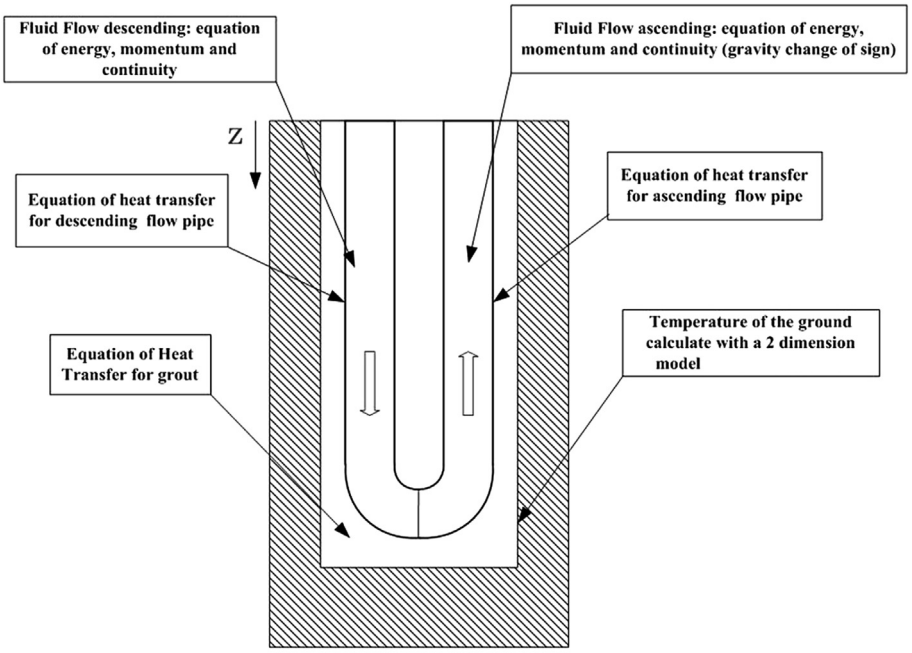

Fig. 3. Diagram of the model.

Table 3
Parameters of the model.

Variables	Values
Length of the descending flow (m)	40
Length of the ascending flow (m)	40
Internal diameter of descending flow (mm)	7.9
Internal diameter of ascending flow (mm)	11.07
External diameter of descending flow (mm)	9.5
External diameter of ascending flow (mm)	12.7
Initial ground temperature (K)	287.5
Diameter of the borehole (m)	0.076
Distance between pipes (m)	0.02
Pipe thermal conductivity (W/m.K)	401
Pipe Specific heat (J/kg.K)	385
Pipe density (kg/m^3)	1000
Grout thermal conductivity (W/m.K)	1.6
Grout specific heat (J/kg.K)	800
Grout density (kg/m^3)	2300
Ground thermal conductivity((W/m.K)	2.8
Ground specific heat (J/kg.K)	600
Ground density (kg/m^3)	2000
Inclination of the evaporator	$\pi/2$

$$\begin{aligned}\mathrm{Titre}(h,P) = {} & \mathrm{flc2hs}(h-\mathrm{hf}(P),0.01)*\mathrm{flc2hs}(\mathrm{hg}(P)-h,0.01)*\\ & \times (h-\mathrm{hf}(P))/(\mathrm{hg}(P)-\mathrm{hf}(P))\\ & + \mathrm{flc2hs}(h-\mathrm{hg}(P),0.01)*0.999\end{aligned}$$

where "flc2hs" is a smoothed Heaviside function predefined in Comsol.

3. Methodology

A standard method was not specifically defined for assessing the refrigerant performance with a direct expansion geothermal evaporator (DX evaporator). However, some methods used to compare the performance of pure and mixed refrigerants in the conventional vapor compression cycle have been developed and used. McLinden and Radermacher [62], for example, evaluated the methods for comparing of pure and mixed refrigerants by computing the COP and the heating capacity for an ideal vapor compression cycle for R22/R114 and R22/R11 mixtures. They conducted investigations using the equal total area method, and optimized the COP by adjusting the relative areas of the evaporator and condenser, while keeping the total heat exchanger area per unit capacity constant.

Although they found that the optimum distribution of the total area varies significantly, the COP exhibits a broad and flat peak versus the fraction of the total area in the evaporator. Also, according to the others [62], if comparisons are based only on one characteristic condensation temperature and one evaporation temperature, then results will depend entirely on how the characteristic temperatures are defined. They concluded that the methods specifying the heat transfer fluid temperatures and a total heat exchanger area per unit capacity are the bests to offer a comparison applicable to both pure and mixed refrigerants. Högberg et al. [63] examined three comparison methods, and the methods differ in how they assess the heat exchange process: (*i*) comparisons between fluids using the equal minimum temperatures approach in the heat exchangers, (*ii*) comparisons between fluids by equal mean temperature differences in the heat exchangers, and (*iii*) comparisons between fluids by equal heat transfer areas. They concluded that to predict, the relations between fluids with a high degree of accuracy, one must use the method with equal heat transfer areas.

Douglas et al. [13] developed a cost-based method for comparing alternative fluids to R22 by defining a single performance index based on the minimum cost for a simplified system operating with a given cooling capacity and efficiency. According to the authors, this method represents an improvement over others for evaluating refrigerants in that it more appropriately considers the influence of both thermodynamic and transport properties on refrigerant choice, and it allows additional costs associated with some replacements (e.g., safety features for flammable refrigerants) to be taken into consideration.

It should be noted that for the different methods listed above, comparisons are made with refrigeration systems with two condensers and evaporators cooled or heated by secondary fluids. Thus, it is easier to set or control the input and output temperatures of the secondary fluids. In a DX GHP that uses the DX evaporator analyzed in this study, there is only one heat exchanger with a secondary fluid: the condenser. As mentioned in the introduction, in the DX evaporator, the refrigerant exchanges heat directly with the ground. Thus, we do not have any control over the evaporation temperature, which also varies greatly due to the pressure drop recorded [10,47]. The means of equal minimum temperatures approach method and equal mean temperature differences method cannot therefore be applied in our case. The cost-based method proposed by Douglas would be very useful for a complete study of the DX GHP, and cannot therefore be used in this study because it concerns only the DX evaporator. Thus, the equal heat transfer area method was selected for use in our work. That means that during the simulation process, we kept constant the length of the DX evaporator, the refrigerant temperature, and the vapor quality at the inlet of the DX evaporator.

Three refrigerants were studied (R22, R407C, R410A) and three comparison cases were examined in this study:

Case #1: Refrigerant temperature (5 °C) and vapor quality (0.2) remain fixed and constant at the DX evaporator inlet and the refrigerant flow rate (0.015 kg.s^{-1}) remains constant in the DX evaporator. The soil temperature is kept constant at 14.5 °C according to our temperature condition.
Case #2: Same as case #1, but with the refrigerant flow rate in the DX evaporator varying.
Case #3: Same as case#1, but with the soil temperature varying.

In all the cases, the thermal performances of the DX evaporator were evaluated by computing the:

- Phase change process
- Pressure drop (Difference between inlet pressure and the outlet pressure of the refrigerant of the evaporator)
- Heat transfer coefficient between the fluid and pipe
- Heat extraction rate from the ground (Ratio between the heat extracted from the ground and the depth of the well)
- Superheating (Difference between the coolant temperature at the outlet of the evaporator and the saturation temperature)

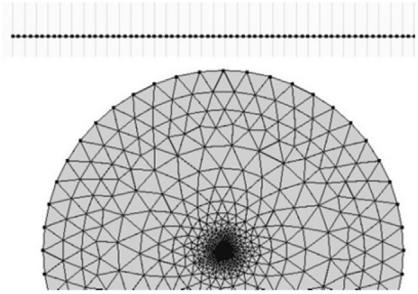

Fig. 5. Meshing of domain.

4. Results and discussion

It should be noted that on the graphics having on the x-axis the borehole length, the data are obtained with a simulation time equal to 450 s (end of simulation). The curves shown are the descending flow from 0 m to 40 m and the ascending flow, which starts from 40 m to 0 m.

According to the conditions described in case #1, the pressure and enthalpy set for the input DX evaporator are about 584 kPa, 246 kJ kg^{-1} for R22, 642 kPa, 250 kJ kg^{-1} for R407C and 936 kPa, 253 kJ kg^{-1} for R410A, respectively. As can be seen, with the same temperature and vapor quality conditions imposed at the evaporators' inlet, the pressure at the inlet of the R410A DX evaporator is approximately 60% higher than that at the R22 DX evaporator inlet and only 10% higher than that at R407C DX evaporator inlet. Resizing the compressor is so need to use R410A as refrigerant for retrofit R22 system.

4.1. Case #1

Figs. 6–8 show the simulation results for this case.

Fig. 6a shows the variation of vapor quality along the DX evaporator with a 40 m depth. From this figure, the phase change extends over 42.5 m for R22 against 52 m and 60 m for R407C and R410A, respectively with a vapor quality of 91.4% for R22, 77.04% for R407C and 69.02% for R410A during the descending flow. We can conclude that the operating conditions are more appropriate for the phase change for R22 than for the two other refrigerants, R407C and R410A, and that those in the R407C DX evaporator are better than that for the R410A DX evaporator. Despite this finding between R410A and R407C, the superheating observed in the R410A evaporator is higher than what is observed with the R407C (Fig. 6b), but is almost the same as that obtained with the R22. However, the advantage with the two fluids replacing R22 is that after 100 s of simulation, the superheating obtained in the operating conditions presented in this study is less than 10 °C. These superheating values

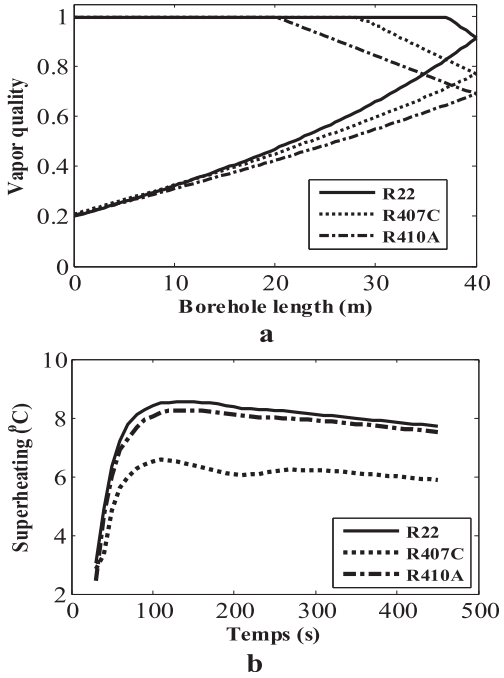

Fig. 6. Vapor quality comparison in borehole (a) and superheating variations comparison (b).

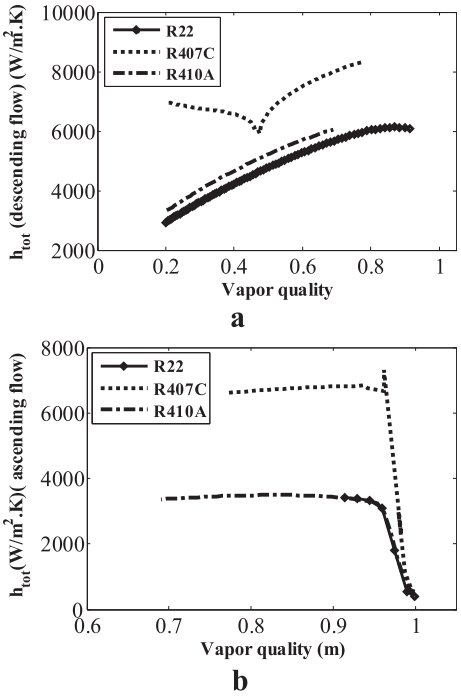

Fig. 7. Heat transfer coefficient comparison.

are favorable for good DX heat pump operation as observed in experimental studies with the DX system [47].

Fig. 7 shows the variations of the global heat transfer coefficient between the refrigerant and the tube wall. Fig. 7a shows the heat transfer coefficient during the descending flow while Fig. 7b shows it in ascending flow. From these figures, it can be noted that during the descending flow, the overall heat transfer coefficient in a DX evaporator increases almost linearly in a range of vapor quality from 0.2 to 0.7 for R22, and 0.2 to 0.8 for R410A along the DX heat exchanger. However, R407C is unique in because a change of the global heat transfer coefficient initially decreases with vapor quality, and then increases, presenting a local minimum in the vapor quality range between 0.4 and 0.6. Note that in the DX evaporator model used, two-phase heat transfer is described by the

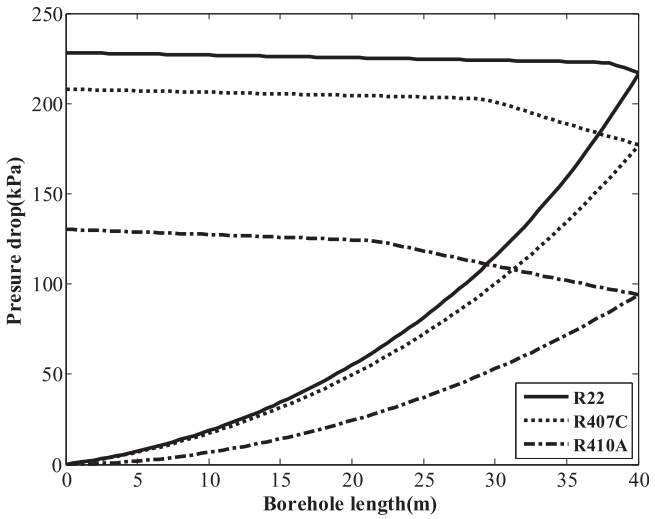

Fig. 8. Pressure drop comparison versus borehole length.

correlation of Chen [61], which results from the interaction between nucleate boiling and liquid convection. When the liquid convection is the main mechanism, the heat transfer coefficient increases with the vapor quality. Indeed, as the flow proceeds downstream and vaporization occurs, the void fraction increases, thus decreasing the density of the liquid–vapor mixture.

As a result, the flow accelerates, enhancing the convective transport from the heated wall of the tube [20]. This is observed in the case of R22 and R410A. In the case of R407C, two regions of heat transfer can be observed, with the first, where nucleate boiling dominates at low vapor qualities. In this region, heat transfer coefficients decrease as the effect of nucleate boiling diminishes. Indeed, as vapor quality increases in annular flow, the effective wall superheat decreases due to a thinner liquid film (less thermal resistance) and to an enhanced convection caused by high vapor velocity. Thus, the number of active nucleation sites decreases until a transition vapor quality is reached. Beyond the transition vapor quality, the effective wall superheat is below the threshold value required for bubble nucleation on the wall. The second region corresponds to convective evaporation. It is characterized by an increase in the heat transfer coefficients with vapor quality as explained previously [20]. During ascending flow, two zones are generally observed: a first area where the heat transfer coefficient remains substantially constant, and a second area where there is a rapid decrease in the heat transfer coefficient corresponding to the end-of-phase change, and where the refrigerant is almost in vapor form. The heat transfer coefficients suddenly drop when the liquid film disappears (for high vapor qualities), leaving the tube wall partially or totally dry because of the low thermal conductivity of the vapor. In all cases, the transfer coefficient in the R407C DX evaporator is greater than that of R410A and R22, with the R410A DX evaporator heat transfer coefficient remaining slightly higher than that of R22 due to its higher thermal conductivity in both the liquid and vapor phases [34]. These observations will help in establishing the simplified relations for the global heat transfer coefficients dependent only on vapor quality for new alternative refrigerants to R22 such as R407C and R410A, for the DX evaporator.

One factor that influences the DX heat pump performance is the pressure drop in the DX evaporator. As can be seen in Fig. 8, and which seems be interesting, the two refrigerant candidates for replacing R22 generate a smaller pressure drop than R22. According to the results, the evaporator pressure drop is about 228 kPa for R22, 208 kPa for R407C, and about 130 kPa for R410A. This is equivalent to a drop of 9% for R407C and 37.4% for R410A, compared to R22. The vapor density of R410A is lower than that of R22, resulting in a lower pressure drop [64]. Moreover, the pressure drop in the R22 DX evaporator remains close to that of R407C because of their similar thermodynamic properties. In addition, as shown in Fig. 8, the pressure drop remains almost constant during the superheating period.

4.2. Case #2

In previous studies on the DXGHP with R22 [47], it has been shown that in the case of DX evaporators in parallel, the misdistribution of refrigerant flow rate can occur and cause an oscillation phenomenon which contributes to lower system performance. That is why this case has been proposed to evaluate refrigerant flow rate impacts. The analysis focused on the effect of the refrigerant flow rate variation on: (*i*) the phase change, (*ii*) the grout temperature, (*iii*) the pressure drop, (*iv*) the superheat, and finally (*v*) the ground heat extracted. The other parameters are kept constant (Table 3). The refrigerant flow rate varies between 0.015 kg s^{-1} and 0.030 kg s^{-1} in steps of 0.05 kg s^{-1}. The pressure and enthalpy set at the evaporator input are those in case #1. Figs. 9–13 show the simulation results obtained in this case.

The general finding for the phase change process (Fig. 9) is that when the refrigerant flow rate increases in the DX evaporator, the evaporation distance also increases. Note that this distance is very important in some heat transfer coefficients during phase changes [65]. The increase in evaporation distance means that the phase change process becomes increasingly difficult. It results in reduced superheating (Fig. 10). In addition, at a low refrigerant flow rate (0.015 kg s^{-1} and 0.020 kgs^{-1}), the phase change process is completed with acceptable superheating (Fig. 9a and b). Conversely, at a high refrigerant flow rate (0.025 kgs^{-1} and 0.030 kgs^{-1}), the phase change process would require more time because more refrigerant mass evaporates, making the process more complex. The result is either an absence or degradation of superheating observed (Fig. 10c and d). It is concluded that these two flow rates do not seem to match the proper operation of the evaporator. The results with the two lowest refrigerant flow rates studied are presented below. Comparing the phase change process for the three refrigerants studied (Fig. 9), we can observe that although, for low refrigerant flow rates (0.015 kgs^{-1} and 0.020 kgs^{-1}), the phase change occurs more quickly in the R407C DX evaporator than that of R410A (Fig. 9a and b). The superheating recorded in the R410A DX evaporator is similar to that of R22 at a 0.015 kgs^{-1} refrigerant flow rate (Fig. 10a). At a 0.020 kgs^{-1} (Fig. 10b) refrigerant flow rate, the superheating produced in the R407C and R410A DX evaporators is less than those produced in the R22 DX evaporator, but after a 200 s simulation, the R410A evaporator reports slightly higher superheating than does the R407C.

In practice, a trade-off should be found between superheating and refrigerant flow rate in order to optimize the DX heat pump performance using this type of evaporator.

Fig. 11 show the pressure drop comparison observed in the evaporators versus what is seen in the borehole length. According to the simulation results, the refrigerant flow rate has a notable influence on the pressure drop in the DX evaporators, and therefore reflects the complex behavior observed in the DX geothermal evaporators, depending on the refrigerant flow rate [10,57]. For the R22 DX evaporator, the largest pressure drop is observed at a refrigerant flow rate of 0.020 kgs^{-1} and in the R410A DX evaporator, the pressure drop increases with an increasing refrigerant flow rate. However, at 0.015 kgs^{-1}, the pressure drop observed in the R22 DX evaporator is still higher than those in the R410A and R407C DX evaporators (Fig. 11a). At a refrigerant flow rate equal to 0.020 kgs^{-1}, the R407C evaporator has a pressure drop greater than those of R22 and R410A (Fig. 11b).

Efforts to optimize the design parameters such as the length, the diameters of the heat exchanger, the refrigerant flow rate, etc., should help reduce this pressure drop and increase the performance of DX evaporators with R407C and R410A.

Table 4 shows the grout cooling values obtained during the simulation, for all refrigerant flow rates. As can be seen, when the flow of the refrigerant in the DX evaporator increases, the grout cooling increases for three refrigerants investigated in this study. However, for low refrigerant flow rates such as 0.015 kgs^{-1} and 0.020 kgs^{-1}, the grout cooling observed in the R410A DX evaporators appears to be higher than those recorded in the R22 and R407C DX evaporators. Grout cooling in the R22 and R407C DX evaporators is at near-similar levels. Note that in the case of R22, the phase change is not complete at a refrigerant flow rate equal to 0.030 kgs^{-1}. This explains the singularity observed on the cooling of grout at this flow rate.

Table 5 depicts the mean values of the heat extraction rate during the simulation. As can be seen, the heat extraction rate increases as the refrigerant flow rate increases for each refrigerant.

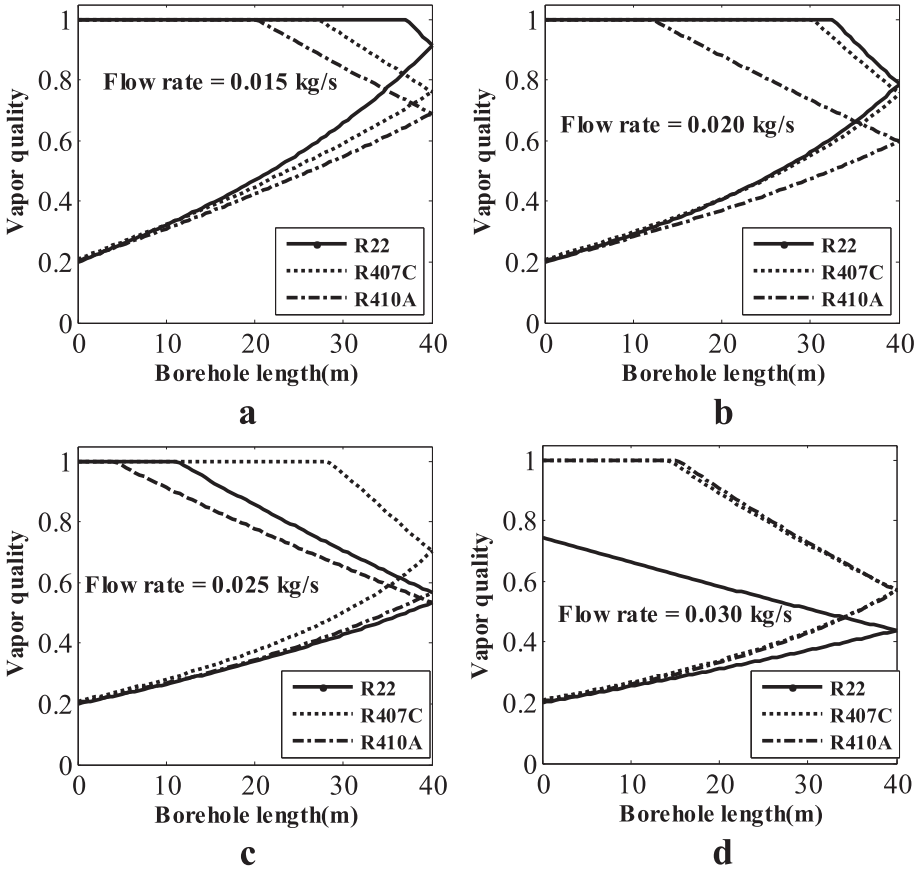

Fig. 9. Vapor quality comparisons versus borehole length.

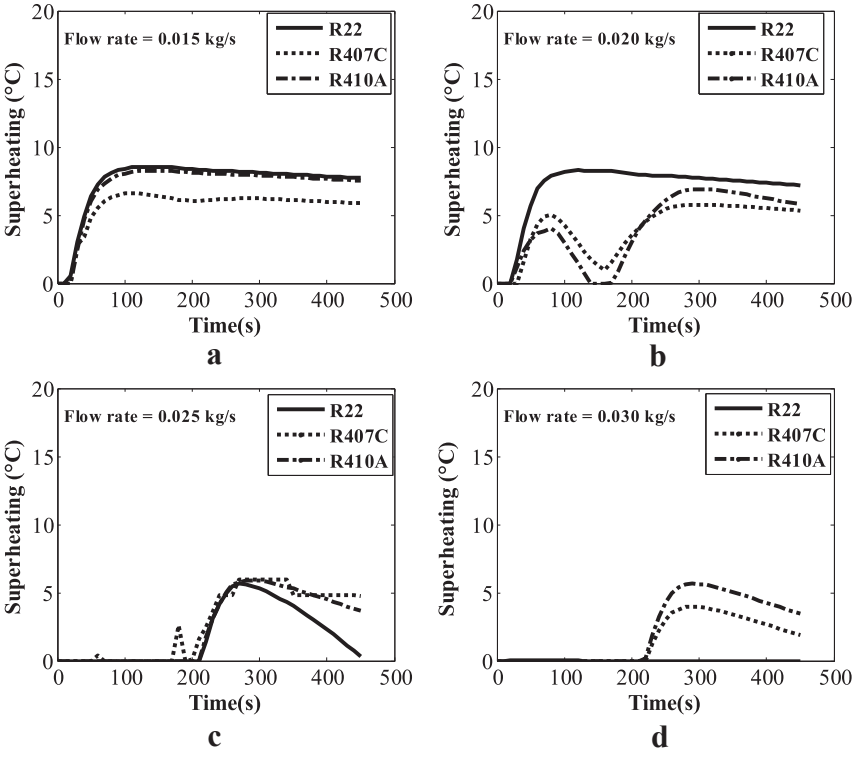

Fig. 10. Superheating variations comparison.

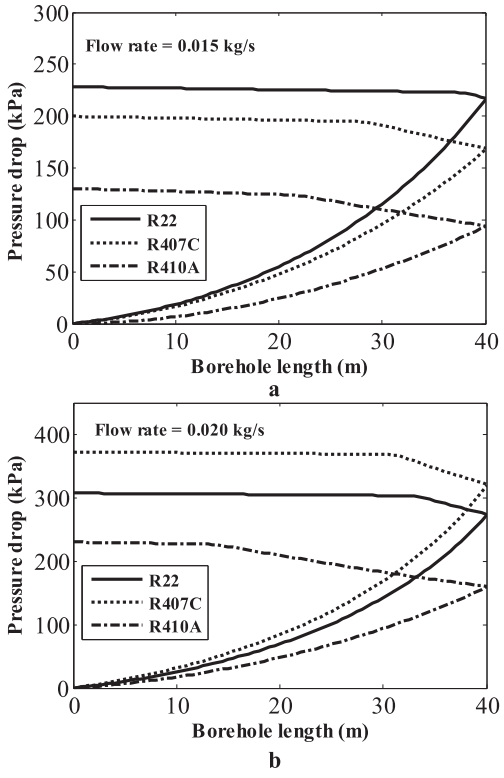

Fig. 11. Pressure drop versus borehole length.

For a given refrigerant flow, from the small differences observed between the HER for the three evaporators, it can be concluded that the HER does not really depend on the type of refrigerants studied, and is therefore an excellent design parameter of DX evaporators. However, the HER for the R410A remains slightly greater or substantially equal to that extracted with R407C. Using the values of R22 (Table 5) as a benchmark, R407C extracts almost the same HER as R22 at 0.015 kg s^{-1} and 0.020 kg s^{-1} refrigerant flow rates, respectively (R410A extracts 3% and 2% more than R22, respectively at 0.015 kg s^{-1} and 0.020 kg s^{-1} refrigerant flow rates). For the refrigerant flow equal to 0.020 kgs^{-1} or more, the mean values of the HER achieved for R407C and R410A (Table 5) remain compatible with the general design values of 45 Wm^{-1} recommended by Percebois [66], and with the European standard EN 15450 Heating System in Buildings-Design of Heat Pump Systems. This standard recommends an HER of 50–60 $W.m^{-1}$ for sizing a DX heat pump installed in a water-saturated sediment [47]. Note that an excessive ground heat extraction can deplete the soil and affect the performance of the geothermal heat pump.

4.3. Case #3

In this section, the influence of soil temperature on the performance of the DX evaporator for R22, R410A and R407C is examined. In the design process of the secondary loop geothermal heat pump, the initial soil temperature is seen in the ground heat exchanger length calculation [67]. Therefore, it is important to analyze the effects of soil temperature on the phase change and on the ground heat extraction rate. In this simplified study, the thermophysical properties of the soil and grout are kept constant, with only the soil temperature varying. The refrigerant pressure, enthalpy and flow rate values at the DX evaporator inlet are those for case 1 for the three refrigerants studied. Note that in the model, the soil temperature here is the initial average temperature around the grout.

Four soil temperatures were evaluated: 10 °C, 13 °C, 15 °C and 20 °C. Fig. 12 presents the vapor quality variations in the DX evaporators as a function of the borehole length for the different soil temperatures. Unlike the increasing effect of the refrigerant flow rate on the phase change in the DX evaporator (case #2), the

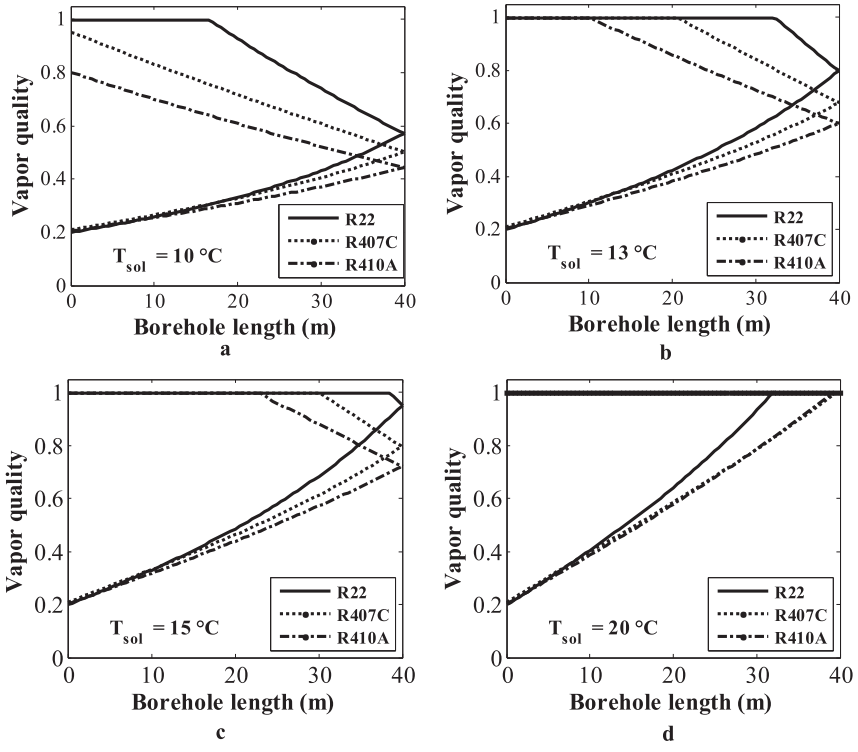

Fig. 12. Vapor quality comparison versus borehole length.

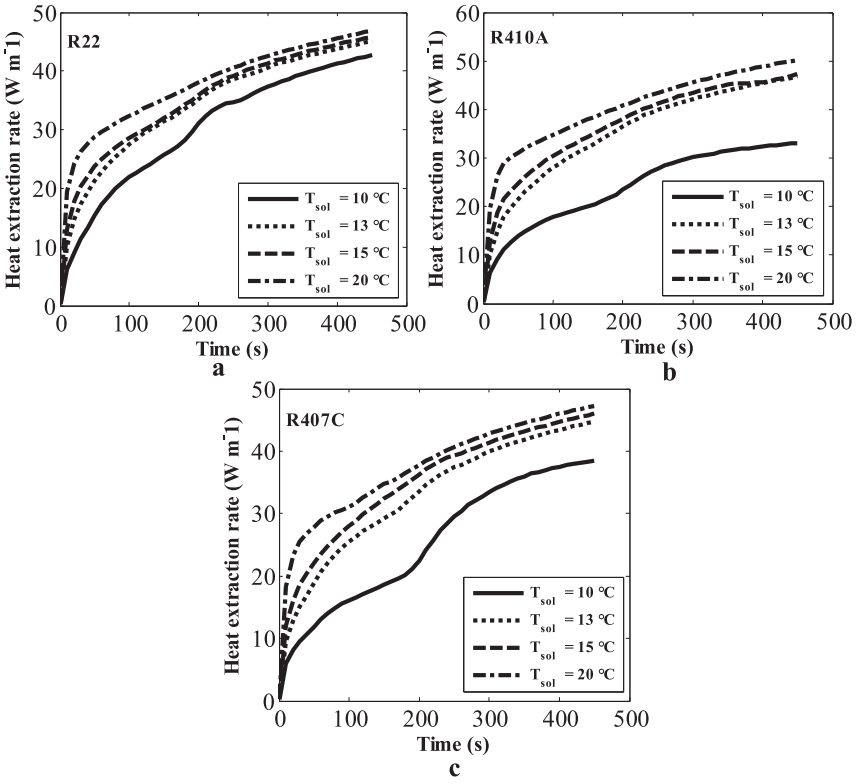

Fig. 13. Heat extraction rate variation for each refrigerant.

increase in the soil temperature accelerates the phase change process in these evaporators by increasing the heat transferred from the soil to the refrigerant. This has the effect of reducing the evaporation distances (Table 6). However, by comparing the behavior of the three evaporators for each soil temperature, we can note that at Ts = 10 °C, the phase change is not completed for the R407C and R410A DX evaporators with vapor quality of 95.1% and 80%, respectively. For soil temperatures above 10 °C, the superheating obtained is between 4 and 13 °C, with the behavior of the R407C DX evaporator which seems to approach that of R22 for soil temperatures above 13 °C. The R410A DX evaporator generates the same superheating (1% less) as that of R22 respectively at T_{sol} = 13 °C, T_{sol} = 15 °C, and about 15% less than that of R22 at T_{sol} = 20 °C, while the R407C DX evaporator generates approximately 29%, 22% and 14% less superheating than that of R22, respectively at T_{sol} = 13 °C, T_{sol} = 15 °C and T_{sol} = 20 C. Between evaporators R410A and R407C DX, the results (Table 6) obtained indicate that the R410A DX evaporator produces superheating about 20%, 26% and 15% more than that of R407C, respectively at T_{sol} = 13 °C, T_{sol} = 15 °C and T_{sol} = 20 °C.

Fig. 13 represents the variation of the heat extraction rate from the ground for each of three refrigerants and for the different soil temperatures. According to the simulation results, it can be noted that when the soil temperature increases, the HER also increases. The R410A DX evaporator seems to have a performance extraction relatively better than that of R22 and R407C. However, comparing the three evaporators for each soil temperature, it can be clearly seen that, for temperatures above 10 °C, the performance of the R407C DX is close to that of R22, and that it would be an excellent retrofit fluid in DX heat pump applications. The values obtained at the end of the simulation for different soil temperatures (Table 6) allow us to conclude that when the phase change is completed, the HER is not really a function of the type of refrigerant because the deviation between the HER values obtained is relatively low. The HER averages are 45.6 Wm^{-1} at T_{sol} = 13 °C, 46.3 Wm^{-1} at T_{sol} = 15 °C and 48.2 Wm^{-1} at T_{sol} = 20 °C with standard deviations of 1.04, 0.6 and 1.8 respectively. As in the previous case, these values are compatible with the HER values recommended for the design proposed by Percebois and the European standard EN 15450 Heating System in Buildings-Design cited above.

5. Conclusion

This study aimed to assess the thermal performance of an R410A and R407C DX evaporator compared to that of R22, which as we know, will be soon eliminated, and to determine what offers the best performance as an R22 replacement in DX heat pumps. At the

Table 4
Cooling of the grout versus refrigerant flow rate.

Refrigerant	Grout cooling (C)			
	Refrigerant flow rate (kgs^{-1})			
	0.015	0.020	0.025	0.030
R22	1.62	2.16	2.37	1.99
R407C	1.61	2.17	2.67	3.0
R410A	1.70	2.22	2.64	3.15

Table 5
Heat extraction rate from the ground.

Refrigerant	Heat extraction rate ($W\ m^{-1}$)			
	Refrigerant flow rate ($kg\ s^{-1}$)			
	0.015	0.020	0.025	0.030
R22	35	46	48	42
R407C	35	46	55	60
R410A	36	47	53	61

Table 6
Evaporation distance, superheating comparison and heat extraction rate.

T_{sol} (°C)	Refrigerant	d_e (m)	Superheating (°C)	HER (Wm^{-1})
10	R22	62	3.4	43.0
	R407C	Not completed	No superheating	38.5
	R410A	Not completed	No superheating	33.0
13	R22	48	6.25	45.0
	R407C	59	4.41	45.0
	R410A	70	5.30	46.8
15	R22	42	8.21	46.0
	R407C	50	6.40	46.0
	R410A	58	8.10	47.0
20	R22	32	13.10	47.0
	R407C	38	11.30	47.3
	R410A	38	13.00	50.2

end of this investigation, the three simulated cases allow allowed the following conclusions:

- At the same inlet temperature, inlet vapor quality and low DX evaporator refrigerant flow rate:
  - ✓ Superheating obtained with R22 and R410A remains similar.
  - ✓ Superheating observed with R407C is acceptable for the proper operation of DX GHP, is but still lower than that obtained for R22 and R410A.
  - ✓ The pressure drop in R22 DX evaporators is higher than those in R407C and R410A.
  - ✓ The pressure drop in R407C DX evaporators is higher than that of R410A.
- Increasing the refrigerant flow rate in the evaporator leads to an increase in the evaporation distance to the three evaporators, and in the possibility of obtaining a liquid at the outlet of the R22 DX evaporator at a high flow rate. The heat extraction rate from the ground remains similar at a given refrigerant flow rate for R410A and R407C.
- When the soil temperature increases, the HER also increases, and does not really depend to the type of refrigerant at a given soil temperature.

Considering similar results between R22 and R410A at low refrigerant flow rates, we can conclude that the R410A can replace R22 in DX heat pumps. However, in this case, the compressor will be resizing to overcome the high discharge pressure. In any case, for the pressure drop observed and recorded superheating in the R407C evaporator compared to those of R22, it can be concluded that R407C is the best fluid for retrofitting R22 systems in the DX GHP. R410A will be very interesting for resized new systems. In all cases, R410A or R407C, optimization efforts are needed to find trade-offs needing to be made between the refrigerant flow rate, the length of the DX heat exchanger, superheating, and pressure drop coupled with experimental studies to develop a more efficient and economical DX systems.

Acknowledgements

Financial support for this study was provided by Natural Resources Canada (Canmet Energy) and the Natural Sciences and Engineering Research Council of Canada (NSERC). The authors would like gratefully to acknowledge their invaluable contributions. In addition, the valuable comments of the reviewers are gratefully acknowledged.

Appendix A. Supplementary data

Supplementary data related to this article can be found at http://dx.doi.org/10.1016/j.applthermaleng.2015.02.079.

References

[1] M.-F. Terrier, Conversion d'une installation du R22 au R404A, Rev. Générale Froid (1997) 41–45.
[2] J.A. Edwards, R.R. Johnson, P. Safemazandarani, Y. Mohammadzadeh, Performance test of a direct expansion heat pump system, in: ASHRAE (Ed.), ASHRAE Transactions, vol. 94, ASHRAE, Dallas, TX, 1998.
[3] J.W. Linton, W.K. Snelson, P.F. Hearty, R.E. Low, B.E. Gilbert, F.T. Murphy, Comparaison of R-407C and R-410A with R-22 in a 10.5 kW (3.0 TR) residential central heat pump, in: P. University, P. e-Pubs (Eds.), International Refrigeration and Air Conditioning Conference, 1996.
[4] Y.H. Guo, G.Q. Zhang, J. Zhou, J.S. Wu, W. Shen, Design and performance of a direct expansion ground-source heat pump system, Chongqing Daxue Xuebao/Journal Chongqing Univ. 34 (2011) 62–66.
[5] P.C. Zhao, G.L. Ding, C.L. Zhang, L. Zhao, Simulation of a geothermal heat pump with non-azeotropic mixture, Appl. Therm. Eng. 23 (2003) 1515–1524.
[6] P.C. Zhao, L. Zhao, G.L. Ding, C.L. Zhang, Experimental research on geothermal heat pump system with non-azeotropic working fluids, Appl. Therm. Eng. 22 (2002) 1749–1761.
[7] R. Yun, J. Hyeok Heo, Y. Kim, Evaporative heat transfer and pressure drop of R410A in microchannels, Int. J. Refrig. 29 (2006) 92–100.
[8] H. Yunho, R. Radermacher, Opportunities with alternative refrigerants, in: Thermal and Thermomechanical Phenomena in Electronic Systems, 2002. ITHERM 2002. The Eighth Intersociety Conference on, 2002, pp. 777–784.
[9] J.M. Calm, D.A. Didion, Trade-offs in refrigerant selections: past, present, and future, Int. J. Refrig. 21 (1998) 308–321.
[10] X. Wang, C. Ma, Y. Lu, An experimental study of a direct expansion ground-coupled heat pump system in heating mode, Int. J. Energy Res. 33 (2009) 1367–1383.
[11] B.T. Austin, K. Sumathy, Parametric study on the performance of a direct-expansion geothermal heat pump using carbon dioxide, Appl. Therm. Eng. 31 (2011) 3774–3782.
[12] Y. Wei, Z. Guoqiang, Z. Jin, W. Haibiao, L. Lin, The design method of U-bend geothermal heat exchanger of DX-GCHP in cooling model, in: Electric Technology and Civil Engineering (ICETCE), 2011 International Conference on, 2011, pp. 3635–3637.
[13] J.D. Douglas, J.E. Braun, E.A. Groll, D.R. Tree, A cost-based method for comparing alternative refrigerants applied to R-22 systems: remplacement du R22: méthode de comparaison des frigorigènes candidats, Int. J. Refrig. 22 (1999) 107–125.
[14] L. Zhao, Experimental evaluation of a non-azeotropic working fluid for geothermal heat pump system, Energy Convers. Manag. 45 (2004) 1369–1378.
[15] S.S. Jadhav, K.V. Mali, Evaluation of a refrigerant R410A as substitute for R22 in window air-conditioner, IOSR J. Mech. Civ. Eng. (2008) 23–32.
[16] K. Nagano, T. Katsura, S. Takeda, Development of a design and performance prediction tool for the ground source heat pump system, Appl. Therm. Eng. 26 (2006) 1578–1592.
[17] J.M. Calm, The next generation of refrigerants – historical review, considerations, and outlook, Int. J. Refrig. 31 (2008) 1123–1133.
[18] E. Cerit, L.B. Erbay, Investigation of the effect of rollbond evaporator design on the performance of direct expansion heat pump experimentally, Energy Convers. Manag. 72 (2013) 163–170.
[19] S. Francois, Système R22: a quels fluides frigorigène les convertir? Technique 714 (2008) 46–51.
[20] A. Greco, Convective boiling of pure and mixed refrigerants: an experimental study of the major parameters affecting heat transfer, Int. J. Heat Mass Transf. 51 (2008) 896–909.
[21] B. Beauchamp, L. Lamarche, S. Kajl, Expemimental evaluation of a direct expansion evaporator using multiple U-tube heat exchangers in parallel, in: VIème Colloque Interuviversitaire Franco-Québecois sur la Thermique des Systèmes, CIFQ, Krakow, Poland, 2009.
[22] C. Rousseau, J.-L. Fannou, L. Lamarche, S. Kajl, Modeling and Analyse of a direct expansion geothermal heat pump (DX) : part 1 modeling of ground heat exchanger, in: Comsol Conference, Boston, USA, 2012.
[23] S.F.Y. Motta, P.A. Domanski, Performance of R-22 and its alternatives working at high outdoor temperatures, in: 8th International Refrigeration Conference at Purde University, P. University, 2000, pp. 47–54.
[24] M.C. Zaghdoudi, S. Maalej, Y. Saad, M. Bouchaala, A comparative study of the performance and environmental characteristics of alternatives to R22 in residential air conditioners for Tunisian market, J. Environ. Sci. Eng. U. S. A. 4 (2010) 37–56.
[25] M. İnallı, H. Esen, Experimental thermal performance evaluation of a horizontal ground-source heat pump system, Appl. Therm. Eng. 24 (2004) 2219–2232.
[26] M. Mohanraj, S. Jayaraj, C. Muraleedharan, Environment friendly alternatives to halogenated refrigerants—a review, Int. J. Greenh. Gas Control 3 (2009) 108–119.
[27] R. Chargui, H. Sammouda, A. Farhat, Geothermal heat pump in heating mode: modeling and simulation on TRNSYS, Int. J. Refrig. 35 (2012) 1824–1832.
[28] D. Jung, C.-B. Kim, S.-M. Hwang, K.-K. Kim, Condensation heat transfer coefficients of R22, R407C, and R410A on a horizontal plain, low fin, and turbo-C tubes, Int. J. Refrig. 26 (2003) 485–491.
[29] Z. Yang, X. Wu, Retrofits and options for the alternatives to HCFC-22, Energy 59 (2013) 1–21.

[30] S.G. Kim, M.S. Kim, S.T. Ro, Experimental investigation of the performance of R22, R407C and R410A in several capillary tubes for air-conditioners, Int. J. Refrig. 25 (2002) 521–531.
[31] Y.A. Kara, Experimental performance evaluation of a closed-loop vertical ground source heat pump in the heating mode using energy analysis method, Int. J. Energy Res. 31 (2007) 1504–1516.
[32] G. Yuefen, T. Roskilly, G. Baker, Z. Honglei, P. Yingxin, Comparison of the thermodynamic performance of direct expansion ground source heat pump using hydrofluoroolefins (HFOs) based on theoretical analysis, in: Power and Energy Engineering Conference (APPEEC), 2012 Asia-Pacific, 2012, pp. 1–5.
[33] J.M. Choi, Y. Park, S.-H. Kang, Heating performance verification of a ground source heat pump system with U-tube and double tube type GLHEs, Renew. Energy 54 (2013) 32–39.
[34] M. Mohanraj, C. Muraleedharan, S. Jayaraj, A review on recent developments in new refrigerant mixtures for vapour compression-based refrigeration, air-conditioning and heat pump units, Int. J. Energy Res. 35 (2011) 647–669.
[35] W. Yang, Experimental performance analysis of a direct-expansion ground source heat pump in Xiangtan, China, Energy 59 (2013) 334–339.
[36] W.-y. Zhang, J. Wei, Analysis on the soil heat accumulation problem of ground source heat pump system in high temperature and high humidity areas, Energy Procedia 14 (2012) 198–204.
[37] B. Rakhesh, G. Venkatarathnam, S.S. Murthy, Experimental studies on a heat pump operating with R22, R407C and R407A: comparison from an energy point of view, J. Energy Resour. Technol. 125 (2003) 101–112.
[38] A.M. Omer, Development and evaluation of a direct expansion heat pump system, J. Adv. Math. 2 (2013) 86–99.
[39] J. Fernández-Seara, A. Pereiro, S. Bastos, J.A. Dopazo, Experimental evaluation of a geothermal heat pump for space heating and domestic hot water simultaneous production, Renew. Energy 48 (2012) 482–488.
[40] C. Montagud, J.M. Corberán, F. Ruiz-Calvo, Experimental and modeling analysis of a ground source heat pump system, Appl. Energy 109 (2013) 328–336.
[41] A. Messineo, V. La Rocca, G. Panno, On-site experimental study of HCFC-22 substitution with HFCs refrigerants, Energy Procedia 14 (2012) 32–38.
[42] H. Wang, Q. Zhao, J. Wu, B. Yang, Z. Chen, Experimental investigation on the operation performance of a direct expansion ground source heat pump system for space heating, Energy Build. 61 (2013) 349–355.
[43] A.M. Omer, Direct expansion ground source heat pump for heating and cooling, Int. Res. J. Eng. 1 (2013) 27–48.
[44] S. Karagoz, M. Yilmaz, O. Comakli, O. Ozyurt, R134a and various mixtures of R22/R134a as an alternative to R22 in vapour compression heat pumps, Energy Convers. Manag. 45 (2004) 181–196.
[45] J.M. Choi, Y.-J. Park, S.-H. Kang, Temperature distribution and performance of ground-coupled multi-heat pump systems for a greenhouse, Renew. Energy 65 (2014) 49–55.
[46] P. Eslami-Nejad, M. Ouzzane, Z. Aidoun, Modeling of a two-phase CO_2-filled vertical borehole for geothermal heat pump applications, Appl. Energy 114 (2014) 611–620.
[47] J.-L. Fannou, C. Rousseau, L. Lamarche, K. Stanislaw, Experimental analysis of a direct expansion geothermal heat pump in heating mode, Energy Build. 75 (2014) 290–300.
[48] W. Chen, A comparative study on the performance and environmental characteristics of R410A and R22 residential air conditioners, Appl. Therm. Eng. 28 (2008) 1–7.
[49] T. Sivasakthivel, K. Murugesan, H.R. Thomas, Optimization of operating parameters of ground source heat pump system for space heating and cooling by Taguchi method and utility concept, Appl. Energy 116 (2014) 76–85.
[50] J.-L.C. Fannou, C. Rousseau, L. Lamarche, S. Kajl, Modeling of a direct expansion geothermal heat pump using artificial neural networks, Energy Build. 81 (2014) 381–390.
[51] Z. Liu, X. Li, H. Wang, W. Peng, Performance comparison of air source heat pump with R407C and R22 under frosting and defrosting, Energy Convers. Manag. 49 (2008) 232–239.
[52] H.-Y. Zhang, J.-M. Li, N. Liu, B.-X. Wang, Experimental investigation of condensation heat transfer and pressure drop of R22, R410A and R407C in mini-tubes, Int. J. Heat Mass Transf. 55 (2012) 3522–3532.
[53] M. Fatouh, T.A. Ibrahim, A. Mostafa, Performance assessment of a direct expansion air conditioner working with R407C as an R22 alternative, Appl. Therm. Eng. 30 (2010) 127–133.
[54] R. Reinhard, H. Yunho, Introduction, in: Vapor Compression Heat Pumps with Refrigerant Mixtures, CRC Press, 2005, pp. 1–16.
[55] S.F. Yana Motta, P.A. Domanski, Performance of R-22 and its alternatives working at high outdoor temperatures, in: 8th International Refrigeration Conference at Purde University, USA, 2000, pp. 47–54.
[56] Y. Guo, G. Zhang, J. Zhou, J. Wu, W. Shen, A techno-economic comparison of a direct expansion ground-source and a secondary loop ground-coupled heat pump system for cooling in a residential building, Appl. Therm. Eng. 35 (2012) 29–39.
[57] B. Beauchamp, Modeling and Experimental Validation of a Direct Expansion Geothermal Heat Pump in: Génie Mécanique, Ph.D thesis, École de Technologie Supérieure, Unniversité du Québec, CANADA, 2011, p. 473.
[58] J.-L. Fannou, C. Rousseau, L. Lamarche, K. Stanislaw, in: SFGP (Ed.), Optimisation d'une pompe à chaleur géothermique à expansion directe (DX) par la méthode Taguchi, vol. 104, 2013. France.
[59] C. Rousseau, J.-L. Fannou, L. Lamarche, M. Ouzzane, Modeling and analyse of a direct expansion geothermal heat pump (DX) : part 1 modeling of ground heat exchanger, in: Comsol Conference Boston, USA, 2012.
[60] B. Beauchamp, L. Lamarche, S. Kajl, A Numerical model of a U-tube vertical ground heat exchanger used as an evaporator, J. Energy Power Eng. 7 (2013) 237–249.
[61] ASHRAE Handbook – Fundamentals (SI Edition), 2009.
[62] M.O. McLinden, R. Radermacher, Methods for comparing the performance of pure and mixed refrigerants in the vapour compression cycle, Int. J. Refrig. 10 (1987) 318–325.
[63] M. Högberg, L. Vamling, T. Berntsson, Calculation methods for comparing the performance of pure and mixed working fluids in heat pump applications, Int. J. Refrig. 16 (1993) 403–413.
[64] R. Prapainop, K.O. Suen, Effects of refrigerant properties on refrigerant performance comparison: a review, Int. J. Eng. Res. Appl. (IJERA) 2 (2012) 486–493.
[65] S. Koyama, A. Miyara, H. Takamatsu, T. Fujii, Condensation heat transfer of binary refrigerant mixtures of R22 and R114 inside a horizontal tube with internal spiral grooves, Int. J. Refrig. 13 (1990) 256–263.
[66] J. Percebois, in: Eyrolles (Ed.), The Guide of Geothermal Heating, 2011.
[67] ASHRAE, Geothermal energy, in: ASHRAE Applications Handbook, 2003.